A pro-inflammatory function of toll-like receptor 2 in the retinal pigment epithelium as a novel target for reducing choroidal neovascularization in age-related macular degeneration

Lili Feng[1@], Meihua Ju[2A], Kei Ying Lee[2A], Ashley Mackey[1], Mariasilvia Evangelista[1], Daiju Iwata[2A], Peter Adamson[2], Kameran Lashkari[1], Richard Foxton[2A], David Shima[2A] and Yin Shan Ng[1#]

[1]*The Schepens Eye Research Institute, 20 Staniford Street, Boston, MA 02114,* [A]*Ocular Biology & Therapeutics,* [2]*UCL Inst. of Ophthalmology, 11-43 Bath Street, London, EC1V 9EL, UK*

[#]Ng; corresponding author: The Schepens Eye Research Institute, 20 Staniford Street, Boston, MA 02114, eric_ng@meei.harvard.edu, telephone: 617-912-2500, fax: 617-912-0128, ORCID 0000-0002-4982-1999

[@]Current affiliations: Lili Feng, Department of Ophthalmology, EYE and ENT Hospital of Fudan University, 83 Fenyang Road, Shanghai, 200031, China; Meihua Ju, Toxikon Corporation, 15 Wiggins Avenue, Bedford, MA 01730, USA; Richard Foxton, NORD Ophthalmology, Roche Pharma Research & Early Development, Roche Innovation Center Basel, F. Hoffmann-La Roche Ltd, Grenzacherstrasse 124, 4070 Basel, Switzerland

Pages: 32; **Tables**: 0, **Figures**: 8

Running title: Anti-TLR2 reduces CNV in AMD

Funding: This project was supported by the BrightFocus Foundation AMD Research Grant M2015214 and by the NIH National Eye Institute Core Grant P30EY003790.

Conflicts of Interest: None

Abstract

Current treatments for choroidal neovascularization, a major cause of blindness for patients with age-related macular degeneration, treat symptoms but not the underlying causes of the disease. Inflammation has been strongly implicated in the pathogenesis of choroidal neovascularization, and in this study we examined the inflammatory role of toll-like receptor 2 (TLR2) in age-related macular degeneration. TLR2 was robustly expressed by the retinal pigment epithelium in mouse and human eyes, both normal and with macular degeneration/choroidal neovascularization. Nuclear localization of NF-κB, a major downstream target of TLR2 signaling, was detected in the retinal pigment epithelium of human eyes, particularly in those with advanced stages of age-related macular degeneration. TLR2 antagonism effectively suppressed initiation and growth of spontaneous choroidal neovascularization in a mouse model, and the combination of anti-TLR2 and anti-vascular endothelial growth factor receptor 2 yielded an additive therapeutic effect on both area and number of spontaneous choroidal neovascularization lesions. Lastly, in primary human fetal retinal pigment epithelium cells, ligand binding to TLR2 induced robust expression of pro-inflammatory cytokines, and end products of lipid oxidation had a synergistic effect on TLR2 activation. Our data illustrate a functional role for TLR2 in the pathogenesis of choroidal neovascularization, likely by promoting inflammation of the retinal pigment epithelium, and validate TLR2 as a novel therapeutic target for reducing choroidal neovascularization.

Introduction

Investigations into the pathophysiology of age-related macular degeneration (AMD) have yielded valuable molecular targets for the treatment of choroidal neovascularization (CNV), including vascular endothelial growth factor A (VEGF)[1, 2]. Although anti-VEGF treatment effectively suppresses the vascular hyperpermeability associated with CNV, this treatment mainly addresses a disease endpoint rather than the molecular mechanism of CNV development[3]. Experimental overexpression of VEGF by either the retina or the RPE in different mouse models did not result in the development of CNV[4-7], suggesting that pathological stimuli in addition to elevated VEGF are required for CNV pathogenesis, and anti-VEGF therapy has critical limitations. Patients receiving anti-VEGF therapies require intraocular injections every 4-8 weeks, potentially lifelong, to maintain their vision[8]. The beneficial effects of anti-VEGF therapy appear to diminish after the third or fourth year of treatment[9-11], and a significant proportion of patients with CNV do not respond to anti-VEGF therapy[12]. Finally, there is emerging evidence that chronic VEGF neutralization may lead to ocular side effects[13-15]. Thus, there is a clear imperative for an alternative therapy that will intervene earlier in the disease process and provide a means for more-effective, long-term management of AMD.

Dysregulated inflammation may play a critical role in the development of AMD[16], and some observations suggest autoimmune contributions[17]. Numerous studies point to involvement of the innate immune system, including interactions among the complement system[18-21], leukocytes[22-25] and pattern recognition receptors such as the toll-like receptors (TLRs)[26, 27], in AMD and CNV[28]. The TLRs are pattern recognition receptors that can bind to and sense both pathogen-associated molecular patterns (PAMPs) and self-derived danger-associated molecular patterns (DAMPs), then mediate appropriate inflammatory and repair responses[26, 29]. TLR2 is expressed primarily on plasma membranes and is essential for the recognition of

microbial lipopeptides (PAMPs) as well as end products of lipid oxidation (DAMPs)[30, 31]. The ω-(2-carboxy-ethyl) pyrrole (CEP) adducts, end products of lipid oxidation, are reportedly endogenous ligands for TLR2 and have been shown to promote angiogenesis in a wound healing model by directly activating TLR2 on endothelial cells[31, 32].

Microenvironments with high oxidative stress, including the highly metabolically active neural retina[33], promote lipid oxidation and formation of CEP adducts. This could result in chronic TLR2 activation, inflammation and, eventually, angiogenesis. Interestingly, there is evidence that CEP adducts and DAMPs in general do not directly activate TLR2, but instead potentiate the activation of TLR2 by PAMPs[34, 35]. This suggests that direct TLR2 activation by pathogens, coupling with potentiation or priming of the TLR2 activity by DAMPs, could be important in the pathogenesis of CNV. Indeed, TLR2 activation by *Chlamydia pneumoniae* has been shown to enhance the expansion of laser-induced CNV[36]. Increased TLR2 expression and reactivity in peripheral blood mononuclear cells from patients with AMD supports the concept that TLR2 may be involved disease pathogenesis[37] and, intriguingly, *C. pneumoniae* was detected in human CNV samples but not in control eyes without AMD[38], highlighting a potential role for pathogen-mediated TLR2 activation in pathology.

In this study, we investigated the expression of TLR2 in human AMD at different stages, including CNV, as well as in age-matched controls without disease to assess potential involvement of TLR2 in AMD pathogenesis. To examine the functional role of this receptor in the initiation and growth of pathological choroidal vessels, neutralizing antibodies against TLR2 were used in a mouse model of spontaneous CNV. Mechanisms for TLR2 activation were examined by treating human primary RPE cells with a combination of different synthetic and natural bacterial ligands, as well as CEP adducts. Results of these studies suggest that

dysregulated TLR2 activation in the RPE may play an important role in the pathogenesis of CNV by modulating the inflammatory response of the RPE. These studies point to the TLR2 pathway as a potential therapeutic target to prevent blindness in patients with AMD.

Materials and Methods

Immunohistochemistry of human tissues

Formalin-fixed and paraffin-embedded sections from de-identified human donor eyes, with (77-90 years old) and without (77 years old) AMD, were deparaffinized in 100% xylene, rehydrated in a series of ethanol, and washed in PBS. Sections were processed for immunohistochemistry using the following antibodies: anti-TLR2 (1:500; Abcam, Cambridge, MA), nuclear factor-κB p65 (NF-κB p65, 1:300; Cell Signaling, Danvers, MA), and control IgGs (goat IgG at 1:500 or rabbit IgG at 1:300; Sigma-Aldrich, St. Louis, MO). Epitope retrieval was accomplished in boiling citrate buffer (pH6). Sections were incubated in 3% H_2O_2 in methanol to inhibit endogenous peroxidases, then blocked in protein blocking solution and incubated in primary antibody overnight at 4°C. The following day, sections for TLR2 staining were incubated in a goat probe for 15 min followed by alkaline phosphatase-polymer that conjugates to the probe (Goat-on-Rodent AP-polymer kit; Biocare Medical, Concord, CA) for 30 min and then visualized with the Vulcan Fast Red chromogenic substrate kit (FR805; Biocare Medical). For NF-κB p65 staining, sections were incubated in MACH2 Rabbit HRP-polymer (Biocare Medical) for 30 min and then visualized with the Deep Space Black Chromogenic substrate kit (BRI4015, Biocare Medical). Finally, the slides with (for TLR2) and without (for NF-κB p65) hematoxylin counterstaining (Gill no.3 hematoxylin, Sigma-Aldrich) were mounted with Permount medium (Thermo Fisher Scientific, Waltham, MA) before imaging using an Axioskop 2 MOT Plus microscope (Carl Zeiss Inc., Thornwood, NY) equipped with an Axiocam

MRc color camera (Carl Zeiss Inc.). Axiovision 4.9.1 (Carl Zeiss Inc.) was used for image acquisition.

Animals

Six-week-old male wild type C57BL/6J mice were obtained from Harlan UK Ltd., (Blackthorn, UK) or the Jackson Laboratory (Bar Harbor, ME, USA), and the JR5558 mice displaying spontaneous CNV[39, 40] were produced from an in-house colony. The animals were fed standard lab chow, received water ad libitum, and were housed in a temperature-controlled environment with a 12-hour day-night cycle. For *in vivo* procedures, mice were anesthetized with a single i.p. injection of a mixture of medetomidine hydrochloride (1 mg/kg body weight; Domitor; Pfizer Animal Health, New York, NY) and ketamine (60 mg/kg body weight, Fort Dodge Animal Health Ltd, Southampton, UK) in sterile water. Prior to procedures involving fluorescein imaging, pupils were dilated with one drop each of 2.5% phenylephrine hydrochloride (Chauvin Pharmaceuticals Ltd, Kingston-Upon-Thames, UK) and 1% tropicamide (Bausch and Lomb, Surrey, UK). After the procedures, an i.p. injection of Antisedan® (20%, Orion Pharma, Espoo, Finland) at 0.01 ml/150 g was used to reverse the effects of the anesthesia. All animal procedures were reviewed and approved according to the British Home Office Animals Scientific Procedures Act 1986 and were performed in accordance with European Directive 86/609/EEC and the ARVO Statement for the Use of Animals in Ophthalmic and Vision Research.

Treatment of spontaneous CNV in JR5558 mice

JR5558 mice[39-41], which spontaneously generate CNV lesions, were treated with a single intravitreal injection (in 0.8 µl) of rat anti-mouse VEGF receptor-2 (VEGFR2) blocking antibody (0.8 or 4.8 µg per injection, MAB4431, R&D systems), purified mouse neutralizing anti-mouse TLR2 antibody (0.8, 1.6, or 3.2 µg per injection, mab-mTLR2, Invivogen), a combination of anti-VEGFR2 and anti-TLR2 antibodies (0.8 +

0.8 μg or 4.8 + 3.2 μg per injection), a mixture of a rat non-immune, isotype-matched control IgG2α antibody (4.8 μg per injection, R&D systems), mouse isotype-matched control IgG1 antibody (3.2 μg per injection, Invivogen), or vehicle control at postnatal day (P) 24. CNV was analyzed by fundus fluorescein angiography (FFA) on P31, seven days after injection, and eyes were collected at 24 hours after FFA for immunohistological analysis. Each litter was divided into at least three different treatment groups, including either a vehicle or control IgG group, to minimize the potential inter-litter variation of responses to the different treatments. Mice (P24) of both sexes were used for the experiments, and at least eight mice were used per treatment group based on prior pilot experiments using the same models. All dosing was done in a masked fashion.

FFA and image analysis for CNV lesions in mice

Analysis of the CNV was performed as described[39,40]. Briefly, the pupils of mice were dilated with 2.5% phenylephrine hydrochloride and 1% tropicamide, then 2% fluorescein sodium (at 10 ml/kg body weight) diluted in water was administered by i.p. injection. Fluorescein angiograms were captured using a Kowa Genesis-Df fundus camera (Kowa, Tokyo, Japan) at early (90 sec after fluorescein injection) and late (7 min post-injection) phases of dye transit. At the early phase, the CNV tissue was clearly defined by the intravascular fluorescein dye whereas at the late phase, extravascular fluorescein was evident as patches of hyperfluorescence. To determine the number of spontaneous CNV lesions per eye in the JR5558 mice, early phase FFA images with the best coverage of the posterior pole (with optic disc at the center) were used. Image J (version 1.48, National Institutes of Health, Bethesda, MD, *http://rsbweb.nih.gov/ij*) was used to quantify CNV area by measuring the areas of hyperfluorescence in late phase FFA images, which correlate well with CNV area based on immunohistologial analysis[39,40]. Animals were excluded for FFA analysis if a clear image of the retina could not be obtained, for example because of

cataracts. All FFA image analysis was performed by trained investigators who were masked to the identity of the treatment groups.

Immunohistological analysis of eye from mice

Eyes were enucleated and fixed with 4% paraformaldehyde in PBS for 3 hr at 4°C. To generate eye sections, the cornea and lens were removed after fixation, and the resulting eye cups with retina were cryoprotected in 30% sucrose in PBS overnight at 4°C, snap-frozen in optimum cutting temperature compound (TissueTek; Sakura Finetek, Torrance, CA) and cryostat sections (10 µm) thaw-mounted onto glass slides. Eyecups whole-mounted without the retina and eyecup sections with the retina were blocked in buffer containing 0.3% Triton X-100 and 5% FBS in PBS (blocking buffer) for 1 hr at room temperature, then incubated overnight at 4ºC with FITC-isolectin B4 (1:300, Vector, Burlingame, CA) alone or in combination with primary antibodies (all at 1:100 dilution), namely anti-F4/80 (Abcam), anti-TLR2 (Abcam), anti-Ezrin (07130, Thermo Fisher, Pittsburgh, PA) or anti-NFκB p65 (Cell Signaling). After three washes, appropriate secondary antibodies, including anti-rat Alexa Fluor® 594, anti-goat Alexa Fluor® 594, anti-rabbit Alexa Fluor® 488 and anti-rabbit Alexa Fluor® 594 (all 1:300; Life Technologies, Waltham MA), were added and specimens incubated at room temperature for 2 hr. Nuclei were stained with DAPI (Life Technologies). After five washes, the specimens were mounted in 50% glycerol, 50% PBS, 0.04% sodium azide and viewed by epifluorescence (Olympus BX51 microscope, Olympus, Essex, UK) with a Retina SRV camera (QImaging, Surrey BC, Canada) with the following objectives and numerical apertures: 4x, 0.16; 10x, 0.40; 20x, 0.75; 40x, 0.90; 60x, 1.35 (oil), and ImagePro 6.2 (Media Cybernetics, Rockville, MD) was used for image acquisition, or an Axioskop 2 Mot Plus microscope (Carl Zeiss, Inc., Throwood, NY) equipped with an Axiocam MRm monochrome color camera (Carl Zeiss Inc.), and Axiovision 4.9.1 (Carl Zeiss Inc.) was used for image acquisition.

215

216 **Real-time PCR**

217 Mouse eyes were stored in RNAlater (Invitrogen, Grand Island, NY) until RNA was
218 extracted from the retina and the RPE/choroid complex using the RNeasy mini kit
219 (Qiagen, Valencia, CA). For experiments using human fetal RPE cells (hfRPE), total
220 RNA was extracted from cells after indicated treatments using the RNAeasy mini kit
221 (Qiagen). Complementary DNA synthesis was performed using the iSCRIPT kit
222 (BioRad, Hercules, CA), as per the manufacturer's specifications. For real-time PCR,
223 reactions were performed on the LightCycler 480 II (Roche, Indianapolis, IN) or a
224 Realplex^2 real-time PCR machine (Eppendorf, Hauppauge, NY) using 0.5 μM primers
225 and Faststart Universal SYBR Green PCR Master Mix (Applied Biosystems, Grand
226 Island, NY). Relative gene expression was determined using the Δ-Δ-Ct method after
227 normalizing sample loading with the housekeeping gene *HPRT1*. The primer
228 sequences are listed below:

human *HPRT1*	5' CCT GGC GTC GTG ATT AGT GAT 3'
	5' AGA CGT TCA GTC CTG TCC ATA A 3'
human *TLR2*	5' TGG TAG TTG TGG GTT GAA GC 3'
	5' GAC AGA GAA GCC TGA TTG GAG 3'
human *IL1B*	5' ATG CAC CTG TAC GAT CAC TG 3'
	5' ACA AAG GAC ATG GAG AAC ACC 3'
human *IL6*	5' CAA CCT GAA CCT TCC AAA GAT G 3'
	5' ACC TCA AAC TCC AAA AGA CCA G 3'
human *CXCL8*	5' AGA AAC CAC CGG AAG GAA CCA TCT 3'
	5' AGA GCT GCA GAA ATC AGG AAG GCT 3'
human *MCP1*	5' TGT CCC AAA GAA GCT GTG ATC 3'
	5' ATT CTT GGG TTG TGG AGT GAG 3'
human *VEGFA*	5' GGG CAG AAT CATC ACG AAG TG 3'

	5’ ATT GGA TGG CAG TAG CTG CG 3’
mouse *Hprt1*	5’ TCA GTC AAC GGG GGA CATA AA 3’
	5’ GGG GCT GTA CTG CTT AAC CAG 3’
mouse *Tlr2*	5’ CCA GAA GCA TCA CAT GAC AGA 3’
	5’ CAA CTT ACC GAA ACC TCA GAC A3’

Isolation and culture of primary human fetal RPE cells

Human fetal eyes were obtained from Advanced Bioscience Resources, Inc. (Alameda, CA) or Novogenix Laboratories, LLC (Los Angeles, CA). Tissues with a gestational age of 15-20 weeks were used. The tissue was harvested within two hr of death and kept on ice. The eyes were shipped the same day and processed the day of arrival. The time from death to tissue processing was 24 ± 4 hours.

RPE isolation and culture were performed according to published methods[42]. Briefly, intact eye globes were rinsed in antibiotic-antimycotic solution (diluted to 10X, Invitrogen) for 5 min. Antibiotics were rinsed off with PBS and the eyes were transferred to a 10-cm petri dish coated with Sylgard-184 (Dow Corning, Midland, MI) and filled with 5% Miller medium. Excess muscle and connective tissues were removed from around the eyes, then the eyes were bisected at one-third the distance from the eye equator to the anterior surface. Prior to separation of the anterior segment of the eye, the vitreous body was cut to avoid detaching the retina from the RPE. The eyecups were then incubated with dispase-I solution (2 U/ml, Roche Diagnostics, Indianapolis, IN) in 5% Miller medium for 45 min at 37°C, transferred to a petri dish filled with 5% Miller medium, fixed with 27G needles in the silicon padding and dissected into quadrants. The retinas were gently removed with fine forceps and RPE-Bruch’s membrane samples were collected directly into a cold trypsin-EDTA solution. After incubation at 37°C for 15 min, the samples were vigorously shaken to separate the RPE cells from Bruch’s membrane. The cells were

pelleted (1300 rpm, 4 minutes), suspended in Miller medium with 15% serum and seeded onto a tissue culture dish (35mm x 10mm). The medium was replaced after 24 hr with 5% Miller medium and changed every two days. Once cells reached confluence (one to two weeks; passage 0), they were seeded into transwells (12 mm insert, 400 nm pores, Corning Inc., Corning, NY) that were coated with laminin extracellular matrix (Sigma-Aldrich), at 1.5- 2.0 x 10^5 cells/well. Cells at passages 1-3 were used for experiments; they were often pigmented and displayed a transepithelial electrical resistance of at least 500 ohm·cm^2 (EVOM2 Voltohmmeter, World Precision Instruments, Inc., Sarasota, FL) as described{Iacovelli, 2016 #77}.

The synthetic TLR2 ligand PAM2CSK4, neutralizing anti-TLR2 antibody (MAb-mTLR2), anti-TLR1 antibody (Anti-hTLR1-IgG), anti-TLR6 antibody (Anti-hTLR6-IgG) and control mIgG1 were obtained from InvivoGen. The high purity (≥ 98% based on NMR analysis) CEP-dipeptide was obtained from a commercial source as a custom synthesis (Haoyuan Chemexpress Co., Limited, Shanghai, P.R.China). *C. pneumoniae* (gamma-irradiation inactivated bacteria from cell lysate) was obtained from Meridian Life Science, Inc (R02620, Memphis, TN).

Statistical analysis

For the JR5558 spontaneous CNV model, total CNV area per eye and number of CNV lesions per eye were quantified using FFA, and each individual eye was analyzed as an individual data point (*n*). Data from FFA were analyzed using one-way ANOVA followed by a Dunnett's post hoc test to compare the different test groups and dosages to either the control (IgG) or the single treatment group (anti-VEGFR2 at 4.8 µg) as indicated (GraphPad Prism). For real-time PCR analysis using hfRPE transwell culture, each transwell was analyzed as individual data point (*n*). For real-time PCR analysis using eye tissues, each individual eye was analyzed as an individual data point (*n*). PCR data were analyzed using one-way ANOVA followed by a Turkey post hoc test to compare between different test groups as indicated

(GraphPad Prism). For all comparisons, values of $p < 0.05$ were considered statistically significant. Data are shown as mean ± SEM unless otherwise noted. All experiments and data analysis for both animal and cell-based experiments were performed in a masked fashion, and sample size was determined based on prior pilot experiments using the same models.

Results

TLR2 is highly expressed by the RPE in human eyes with and without AMD

In light of the evidence for inflammation as a contributor to AMD and the critical role of TLR2 in modulating oxidative stress-induced angiogenesis in a wound-healing model[31, 32], we investigated the expression of TLR2 in CNV associated with AMD. Robust expression of TLR2 was detected in the RPE at all stages of AMD as well as in the RPE of control eyes with no signs of AMD (Figure 1). Some TLR2-positive endothelial cells and/or leukocytes associated with the vessels were also observed in the choroid, and sometimes a few pigmented cells (likely RPE) within the CNV membrane were positive for TLR2 staining (Figure 1i-j), but interestingly, the CNV membrane (including the vessels) was only weakly stained or negative for TLR2 expression. Weak TLR2 staining was also detected on drusen (Figure 1e-f). These data suggest that RPE cells normally express high levels of TLR2, and that the RPE continue to express TLR2 at different stages of AMD.

RPE cells display greater nuclear localization of the TLR2 target NF-κB during intermediate and late stages of human AMD.

We used immunohistological analysis of clinical specimens to examine nuclear localization of NF-κB, a major downstream target of the TLR2 pathway, as an indicator of TLR2 activation. Nuclear localization of NF-κB was detected in a small number of RPE cells in aged eyes without any signs of AMD and with early AMD,

corresponding to AREDS 1. Greater numbers of RPE cells displaying nuclear translocation of NF-κB were observed in RPE cells in aged eyes with intermediate AMD, corresponding to AREDS 3, and advanced AMD (Figure 2). Activation of NF-κB was detected in some cells in the choroid, likely endothelial cells of the choroidal vessels and resident leukocytes (Figure 2), a pattern similar to that observed for TLR2 (Figure 1). Interestingly, in the CNV membrane and in the adjacent retina, nuclear staining of NF-κB was mostly detected in cells with small rounded nuclei (Figure 2g). These are likely infitrated inflammatory cells, since vascular endothelial cells often have elongated nuclei (Figure 2i-p). The lack of nuclear NF- κB in the CNV membrane (Figure 2g) matches the lack of TLR2 expression in the CNV lesion (Figure 1).

TLR2 is highly expressed by the RPE in mouse eyes with and without CNV

To investigate the role of TLR2 in the pathogenesis of CNV, the JR5558 mouse, an established model of spontaneous CNV[39,40], was used. As with the human eyes, the RPE cells in close proximity to and distant from the CNV lesion were positive for TLR2 staining (Figure 3). RPE cells in the wild type control mouse, too, stained positive for TLR2 (Figure 3d-f). TLR2 was localized to the apical side of the RPE (Figure 3g-j), where it co-localized with ezrin, a marker for RPE microvilli (Figure 3k-m). The vessels of the spontaneous CNV were mostly negative for TLR2 staining, though some cells that tightly associated with the CNV vessels, likely leukocytes and/or microglia, were positive for TLR2 (Figure 3a-c). Immunostaining of the eye sections confirmed the lack of TLR2 staining in CNV vessels (Figure 3g-h).

Using semi-quantitative reverse transcription and real-time qPCR analysis, significantly higher expression levels of *Tlr2* mRNA were detected in the RPE/choroid complex compared to the retina from both the wild-type C57BL/6J and the JR5558

mice (Figure 3n). Taken together, these results suggest that the primary source of TLR2 in the eye is the RPE, both in normal eyes and in eyes with CNV.

TLR2 plays a functional role in CNV development

To determine the function of TLR2 in the development of CNV, including the initiation as well as growth of the CNV lesion, different doses (0.8, 1.6, and 3.2 μg per injection per eye) of TLR2-neutralizing antibody were delivered via a single intravitreal injection into the eyes of JR5558 mice, then the effect on CNV was analyzed by FFA seven days post-injection. All three doses of anti-TLR2 antibody significantly suppressed the formation of CNV, with an efficacy that was similar to that of VEGFR2 neutralization (0.8 and 4.8 μg per intravitreal injection per eye) (Figure 4). The higher doses of anti-TLR2 antibody (1.6 and 3.2 μg) were significantly more effective in reducing the area of CNV per eye compared to the lower dose (0.8 μg), indicating a dose response for the anti-TLR2 antibody in reducing CNV development in this model (Figure 4b). No significant dose effect was observed for the anti-VEGFR2 antibody, suggesting that the 0.8 μg intravitreal dose was already achieving maximal inhibition.

As expected, combination treatment with anti-VEGFR2 and anti-TLR2 antibodies resulted in significant inhibition of the number of CNV lesions per eye as well as CNV area per eye compared to the IgG control. Interestingly, the high-dose combination treatment (4.8 μg anti-VEGFR2 and 3.2 ug anti-TLR2) was significantly better than the high-dose treatment with anti-VEGFR2 alone (4.8 μg) for reducing the number of CNV lesion per eye and in reducing average CNV area per eye (Figure 4b). No significant difference was detected between other combination treatment groups and the anti-VEGFR2 treatment groups. These results suggest an additive suppressive effective for antagonism of VEGFR2 and TLR2 on the development of

spontaneous CNV, and that the VEGFR2 and TLR2 pathways may have non-overlapping function during CNV pathogenesis.

TLR2 promotes macrophage recruitment to the CNV

Because macrophage recruitment to sites of CNV plays a significant role in pathological vessel development in the JR5558 mice[40], the eyes from animals treated with antibodies against VEGFR2 and/or TLR2 were examined by immunohistochemistry to determine the morphology of the CNV vessels and the degree of macrophage association with the CNV. Although there were no obvious morphological differences between the CNV vessels in eyes treated with anti-VEGFR2 and/or anti-TLR2 and those treated with vehicle, the levels of staining for macrophages associated with the CNV were dramatically lower in eyes treated with anti-TLR2 alone or anti-TLR2 in combination with anti-VEGFR2 (Figure 5). Anti-VEGFR2 treatment alone was effective in inhibiting CNV development (Figure 4), but this treatment had no detectable effect on the degree of CNV-associated macrophages (Figure 5). These data suggest that TLR2 activation in the RPE promotes recruitment of macrophages during CNV, and that this effect is independent of that of the VEGF/VEGFR2 pathway.

Activation of TLR2 promotes expression of pro-inflammatory cytokines by the RPE

To determine why TLR2 antagonism was effective in inhibiting spontaneous CNV development and, in particular, macrophage recruitment to the CNV, we determined the effect of TLR2 activation on RPE cells in vitro. Cultured hfRPE expressed *TLR1*, *TLR2*, *TLR4* and *TLR6* mRNA, albeit at levels significantly lower (2- to 16-fold) than those observed for THP-1 cells (data not shown), a human monocyte cell line known to express high levels of these TLRs[43]. Treatment of hfRPE with a synthetic diacylated lipopeptide TLR ligand, Pam2CSK4[44], led to robust induction of the mRNA

for pro-inflammatory cytokines interleukin 6 (*IL6)*, monocyte chemoattractant protein 1 (*MCP1*/*CCL2*), C-X-C motif chemokine ligand 8 (*CXCL8/IL8*), interleukin 1 beta (*IL1B*) and *TLR2* itself. Neutralizing antibody against TLR2 significantly blocked the increase in cytokines/*TLR2* expression induced by Pam2CSK4 (Figure 6a). The degree of up-regulation was variable, likely due in part to the fact that different isolates of hfRPE had different baseline levels of expression for these pro-inflammatory genes, but significant induction was observed in all hfRPE isolates tested (Figure 6).

To determine if other TLRs contribute to the Pam2CSK4-induced expression of pro-inflammatory genes, e.g. via hetero-dimerization with TLR2, neutralizing antibodies against TLR1 and TLR6 were tested both alone and in combination with anti-TLR2 antibody. Only anti-TLR2 neutralizing antibodies were effective in inhibiting Pam2CSK4-induced up-regulation of *IL1B*, *IL6* and *TLR2* in our system (Figure 6b).

End products of lipid oxidation enhance TLR2-mediated expression of pro-inflammatory genes in RPE

We next sought to identify a pathologically relevant ligand that could mediate TLR2 activation in the RPE during AMD pathogenesis. The aged RPE is exposed to high oxidative stress in the lipid-rich microenvironment of the retina and, during AMD, in drusen deposits. End products of lipid oxidation, including CEP adducts, can directly activate TLR2 and promote angiogenesis[31, 32]. We therefore tested the effect of CEP on TLR2 activation in RPE cells.

Primary hfRPE were treated with different doses of Pam2CSK4 and CEP, both alone and in combination, and expression of pro-inflammatory genes was assessed by qPCR. CEP alone did not induce expression of pro-inflammatory cytokines or chemokines in hfRPE (Figure 7), even at doses up to 52.4 μM and duration of treatment of up to 72 hours (data not shown). However, addition of CEP

to Pam2CSK4 significantly enhanced expression of *IL6*, *MCP1*, *CXCL8*, *IL1B* and *TLR2* relative to Pam2CSK4 treatment alone (Figure 7a-c, e,f). Interestingly, treatment with Pam2CSK4 and CEP, either individually or in combination, did not significantly affect expression of *VEGFA* (Figure 7d). These data suggest that CEP is not a conventional ligand for TLR2, but rather functions as a co-stimulatory ligand to potentiate and enhance the activation of TLR2 by conventional ligands such as Pam2CSK4 that regulate expression of pro-inflammatory genes.

Next, we probed the effect of gamma-irradiation inactivated *C. pneumoniae* (Cpn)[36, 38], a bacterial strain associated with AMD on TLR2-mediated expression of pro-inflammatory genes. The effects of Cpn were assessed in the presence or absence of CEP. Combination treatment of hfRPE with Cpn and CEP enhanced expression of *MCP1*, *CXCL8* and *IL1B* compared to Cpn treatment alone at the six- and 48-hour time points (Figure 8c-h). Induction of *IL6* expression by Cpn was also significantly enhanced by CEP treatment at the 48-hour time point (Figure 8a-b). Treatment with a neutralizing anti-TLR2 antibody significantly suppressed induction of the pro-inflammatory genes by the Cpn and CEP combination treatment, confirming that TLR2 is involved in the response. Again, treatment with Cpn and/or CEP did not significantly increase *VEGFA* expression in hfRPE compared to untreated controls (Figure 8i-j). Cpn therefore acts as a ligand for TLR2 in RPE cells, promoting expression of pro-inflammatory genes, and the activity of TLR2 in this context is enhanced by end products of lipid oxidation

Discussion

To validate the functional role of TLR2 in CNV pathogenesis, we examined the expression of TLR2 in clinical specimens and in an animal model of AMD. The finding that RPE cells express high levels of TLR2 on their apical surface is a reflection of RPE function as a barrier, an important role in immune surveillance, as a sensor for various PAMPs and DAMPs in the retina [27, 45]. The increase in nuclear localization of NF-κB with AMD progression could indicate an increase in TLR2 activation and a possible pro-inflammatory function for RPE in AMD pathogenesis. As AMD progresses, the RPE become atrophic, which would result in a reduction in overall TLR2 levels in the eye, due to the loss of RPE. This is consistent with our observation of lower TLR2 staining levels because of RPE loss in the clinical samples with advanced AMD (CNV) compared to eyes with earlier stage AMD or without AMD. This finding is also consistent with the data from the mouse model of spontaneous CNV, in which the levels of TLR2 gene expression by the RPE/choroid complex tended to be lower than those for age-matched, wild-type controls, though this difference was not statistically significant.

Although some TLR2-positive cells were detected in the choroid in both the human and mouse eyes, neovessels in the CNV did not express high levels of TLR2. These finding differ from the reports of TLR2 in endothelial cells, in which TLR2 has been implicated in oxidative stress-modulated angiogenesis during wound healing[31]. This dissimilarity is likely due to the difference in mechanisms of angiogenesis between these two models. We have shown that the spontaneous CNV model is driven by inflammation[39-41] and thus may lack certain components of the oxidative-stress–mediated wound-healing response, which would include TLR2-expressing endothelial cells. Since TLR2 antagonism effectively inhibited the initiation and growth of spontaneous CNV, it is reasonable to assume that TLR2 activation in the RPE plays an early role in CNV pathogenesis. The reduction in CNV-associated

463 macrophage investment observed with anti-TLR2 treatment is consistent with this
464 hypothesis, since macrophage recruitment to the CNV/RPE is considered to be one
465 of the initial steps that drives CNV pathogenesis[28].

466 It was surprising that the CEP adduct, a known component of drusen that has
467 been associated with AMD pathogenesis[46, 47], did not directly activate TLR2 in RPE,
468 though it did enhance the effects of both synthetic and bacterial ligands. By
469 enhancing activation of TLR2 activation by other ligands, CEP generated during
470 aging could exacerbate the TLR2-mediated inflammatory response in the RPE. It is
471 important to point out that hyperactivation of TLR2 by the synthetic ligand or bacterial
472 ligand in combination with CEP in our cell-based model induced NF-κB activation but
473 was not sufficient to induce activation of the inflammasome and RPE cell death (data
474 not shown). However, it did lead to induction of pro-inflammatory genes including *IL-*
475 *1β*, which could represent a priming step necessary for full activation of the
476 inflammasome in the RPE by additional signals, such as oxidative stress or
477 lysosomal destabilization[48]. Thus, we speculate that CNV pathogenesis in aging eyes
478 may involve a two-hit process: the first, accumulation of CEP in aging eyes that
479 effectively sensitizes TLR2 for promoting inflammation; the second, activation of
480 TLR2 by DAMPs and/or PAMPs such as infection with bacteria or viruses. This two-
481 step process would trigger hyperactivation of the TLR2 and chronic RPE-mediated
482 inflammation, resulting in tissue damage, subsequent upregulation of *VEGFA*
483 including by the RPE and recruited macrophages and eventual neovascularization. In
484 support of this concept, *C. pneumoniae* antigen has been detected in clinical
485 samples of CNV membranes, and human cytomegalovirus infection has been
486 associated with wet AMD[38,49, 50]. If this mechanism is responsible for even a portion of
487 CNV pathogenesis, treating patients with broad-spectrum antibiotics and/or anti-viral
488 drugs to suppress infection at the RPE could inhibit the development of CNV and
489 represent a novel means of reducing the incidence and/or progression of CNV.

TLR2 antagonism effectively blocked CNV in our mouse model of spontaneous CNV, either when used as a mono-therapy or in combination with anti-VEGFR2, suggesting that targeting of TLR2 activation could be an efficacious therapeutic strategy for CNV. Although our studies focus on TLR2, it is well established that other TLRs are expressed by the RPE, and some have been implicated in AMD pathogenesis[26-28,32]. It will be important to determine if other TLRs contribute to CNV pathogenesis by promoting RPE inflammation.

Since TLR2 is highly localized on the apical surface of RPE, ocular delivery of TLR2 antagonist could be an effective route of delivery. Furthermore, since the TLR2-null mice are largely normal, and do not display any reported retinal phenotype, ocular TLR2 antagonism for CNV should be relatively safe[36, 51]. TLR2 may therefore serve as a novel therapeutic target for reducing CNV, either as a single therapy or in combination with anti-VEGF therapy for wet AMD.

Acknowledgements

The authors acknowledge the assistance of Shannon Bunker of University College London for the animal dosing and FFA experiments, and Magali Saint Geniez, Jared Iacovelli and Gopalan Gnanaguru of the Schepens Eye Research Institute (SERI) for instruction in culturing primary RPE, and Gianna Teague of SERI for technical advice for immunohistological staining. This project was supported by the BrightFocus Foundation AMD Research Grant M2015214 and by the NIH National Eye Institute Core Grant P30EY003790. Ng is the guarantor of this work and, as such, had full access to all data in the study. He takes responsibility for the integrity of the data and the accuracy of the data analysis. The authors thank Dr. Gerald Gough and Dr. Monica Belich for scientific discussion, Dr. Patricia D'Amore for critical reading of the manuscript and Dr. Anne Goodwin for scientific editing.

LF, MJ, KYL, AM, ME, DI and RF carried out the experiments, collected and analyzed the data, and generated the figures. DS, PA and KL

contributed to experimental design and data interpretation, and provided technical assistance for experiments. YSN conceived, designed and assisted with the experiments, and performed data interpretation, generation of figures and literature searches. All authors were involved in the writing paper and had final approval of the submitted versions.

Figure legends:

Figure 1. Expression of TLR2 (red staining) in the RPE/choroid area of aged eyes (≥ 77 yrs) without AMD and with different stages of AMD. (A, B) Aged eye (77 yrs) without AMD (C, D), aged eye with early AMD (AREDS 1), (E-F) aged eye with intermediate stage AMD (AREDS 3), (G-J) aged eye with advanced AMD, showing regions without CNV (G, H) and with CNV (I, J; green asterisk). Note the absence of the RPE layer beneath regions with CNV. Brm, Bruch's membrane; blue arrows, RPE; black arrowheads, TLR2-positive staining; red V, vessel in CNV; white arrowheads in E-F, a small drusen. IgG Control = isotype match IgG, Bar = 10 μm.

Figure 2. Activation of NF-κB in the RPE during AMD pathogenesis. (A-D) In aged eyes without any signs of AMD and with early AMD (≧ 77 years), only a few RPE cells displayed nuclear localization of NF-κB (white arrows). Cells with nuclear NF-κB staining in the choroid of the eyes with no AMD and with early AMD may be vascular endothelial cells and inflammatory cells (blue arrows in A, C). (E-P) In aged eyes with intermediate AMD and advanced AMD (≧ 77 years), nuclear localization of NF-κB was detected in many RPE cells (white arrows in E, I, K, M, O). In the CNV membrane (green asterisk), staining for nuclear NF-κB was unremarkable and limited to a few cells in the retina (green arrows) and choroid (blue arrows) (G, H). RPE cells

with activated NF-κB were detected near the transition zone with geographic atrophy (outlined with white dotted line) (I, J). The absence of RPE in the area with geographic atrophy could contribute to the lower number of RPE cells with nuclear NF-κB staining near the transition zone. NF-κB–positive cells in the retina (green arrows in G, I, M and O) are likely to be inflammatory cells because of their rounded nuclear morphology. More nuclear NF-κB staining in choroidal cells was detected in eyes with intermediate AMD and advanced AMD (blue arrows in E, I, K, M and O). Brm, Bruch's membrane. Bars in A-H and K-P = 20 μm, bar in I, J = 50 μm.

Figure 3. Expression of TLR2 in the RPE of wild-type C57BL/6J and JR5558 spontaneous CNV mice. (A-F) En face view of whole-mount eyecups (with the retinae removed). Staining shows robust TLR2 expression (red) on the RPE both around and at a distance from the CNV vessels (IB4, green), whereas little TLR2 staining of CNV vessels (IB4, green) was detected in the JR5558 mice (A-C). In the whole-mount eyecups from wild-type C57BL/6J mice, strong TLR2 expression was detected on the RPE (D, E). (G-J) In eye sections from JR5558 mice, expression of TLR2 was detected readily on the apical side of the RPE layer, whereas the CNV vessels (outlined by white dotted oval) were largely negative for TLR2 expression (H). Panels G and H are from a region with CNV whereas I and J are from a CNV-free region, panels H and J are higher magnification images of the boxed areas in panels G and I, respectively. (K-M) Double immunostaining of eye sections from JR5558 mice revealed co-localization of ezrin (green), a marker for microvilli of RPE, and TLR2 (red) to the apical surface of the RPE layer. ONL = outer nuclear layer of the photoreceptors. Bar for A-C = 50 μm, for D-F = 20 μm, for G and I = 100 μm, for H and J = 50 μm, for K-M = 50 μm. (n) Semi-quantitative qPCR for TLR2 mRNA levels in both wild-type C57BL/6J and JR5558 mice, showing significantly higher levels of TLR2 mRNA in the RPE/choroid complex compared to the retina. Data = mean ± SEM, *P < 0.05, ***P < 0.001 by one-way ANOVA.

572

573 Figure 4. Intravitreal anti-TLR2 neutralizing antibody significantly suppresses
574 spontaneous CNV initiation and growth. (A) Representative FFA images showing the
575 CNV lesions (hyper-fluorescent spots, asterisks) in different treatment groups. Note
576 the substantial reduction in the number of CNV lesions in the anti-VEGFR2 and anti-
577 TLR2 combination treatment groups. (B) Quantification of the FFA data from A,
578 showing a significant reduction in the average number of CNV lesions per eye as
579 well as the average CNV area per eye in the anti-VEGFR2 groups and the anti-TLR2
580 groups, both as individual treatment and as combination treatment. IgGs = rat IgG2A
581 at 4.8 μg and mouse IgG1 at 3.2 μg per injection. Data = mean +/- SEM, n (eye) = 12
582 to 33. **P < 0.01, ***P < 0.001 compared to IgG control-treated group, one-way
583 ANOVA. †P < 0.05, ††P < 0.01 comparing the different treatment groups as
584 indicated, one-way ANOVA.

585

586 Figure 5. TLR2 antagonism in the eye reduces macrophage association with CNV in
587 the JR5558 mouse. Representative images of macrophage staining using whole-
588 mount eyecups without retinae from all treatment groups. Whereas both anti-
589 VEGFR2 and anti-TLR2 treatments effectively suppressed growth of CNV vessels,
590 only anti-TL2 treatment reduced the number of CNV-associated macrophages
591 (F4/80, red) in the eye. Macrophages and their nuclei in the Vehicle group are
592 highlighted with white arrows, whereas some of the RPE cells and their nuclei are
593 highlighted with white triangles. IB4; vascular staining (green), bar = 200 μm.

594

595 Figure 6. TLR2 mediates expression of pro-inflammatory genes in primary human
596 RPE cells. (A) Pam2CSK4, a synthetic diacylated lipoprotein and TLR2-selective
597 ligand, induced robust expression of *IL6*, *MCP1*, *CXCL-8*, *IL1B*, and *TLR2* by primary
598 human RPE cells, an induction that was suppressed by a TLR2-specific neutralizing
599 antibody (4 μg/ml). (B) Induction of *IL1B*, *IL6* and *TLR2* expression in human primary

RPE cells by Pam2CSK4 was not affected by neutralizing antibodies against TLR1 (4 μg/ml) or TLR6 (4 μg/ml). Data = mean ± SEM, *P < 0.05, **P < 0.01, ***P < 0.001, one-way ANOVA. Note that at least two different donor eyes were used for primary human RPE isolation and culture for this experiment.

Figure 7. Carboxyethylpyrrole (CEP)-dipeptide has a significant synergistic effect with the TLR2-selective ligand Pam2CSK4 on inducing expression of pro-inflammatory genes in human primary RPE cells. (A-C, E-F) CEP alone did not induce the expression of *IL6*, *MCP1*, *CXCL8*, *IL1B*, or *TLR2*, whereas Pam2CSK4 significantly induced expression of these genes in hfRPE. Combination treatment with CEP and Pam2SCK4 resulted in a synergistic induction of these pro-inflammatory genes, and anti-TLR2 neutralizing antibody (4 μg/ml) significantly suppressed the effects of the CEP and Pam2CSK4 combination treatment. (D) CEP, Pam2CSK4, and the combination failed to induce *VEGFA* expression compared to the control in hfRPE cells. A-D = 100 ng/ml (78.6 nM) of Pam2CSK4, E-F = 50 ng/ml (39.3 nM) of Pam2SCK4. CEP was used at 10 μg/ml (26.2 μM) for A-F. Data = mean ± SEM, *P < 0.05, **P < 0.01, ***P < 0.001, one-way ANOVA.

Figure 8. Synergistic effects of CEP-dipeptide with gamma irradiation-inactivated *Chlamydia pneumoniae* (Cpn) in inducing TLR2-mediated expression of pro-inflammatory genes in RPE cells. Primary hfRPE cells were treated with Cpn (100 μg/ml) alone or Cpn plus CEP (26.2 μM) for either 6 hours (A, B, C, D, E) or 48 hours (F, G, H, I, J). A synergistic effect for *IL6* expression was detected at the 48 hours, whereas synergistic effects for the expression of *MCP1*, *CXCL8* and *IL1B* were detected at both 6 and 48 hours. The induction of expression of pro-inflammatory genes by treatment with Cpn and CEP was significantly suppressed in the presence of an anti-TLR2 neutralizing antibody (4 μg/ml) (A-D, F-I). Treatment with Cpn either alone or in combination with CEP did not induce *VEGFA* expression in hfRPE at 6 or

48 hours compared to control. Anti-TLR2 antibody significantly suppressed background VEGF expression in the control group at 6 hours and in the group treatment with Cpn plus CEP at 48 hours (E, J). Data = mean ± SEM, *P < 0.05, **P < 0.01, ***P < 0.001, one-way ANOVA.

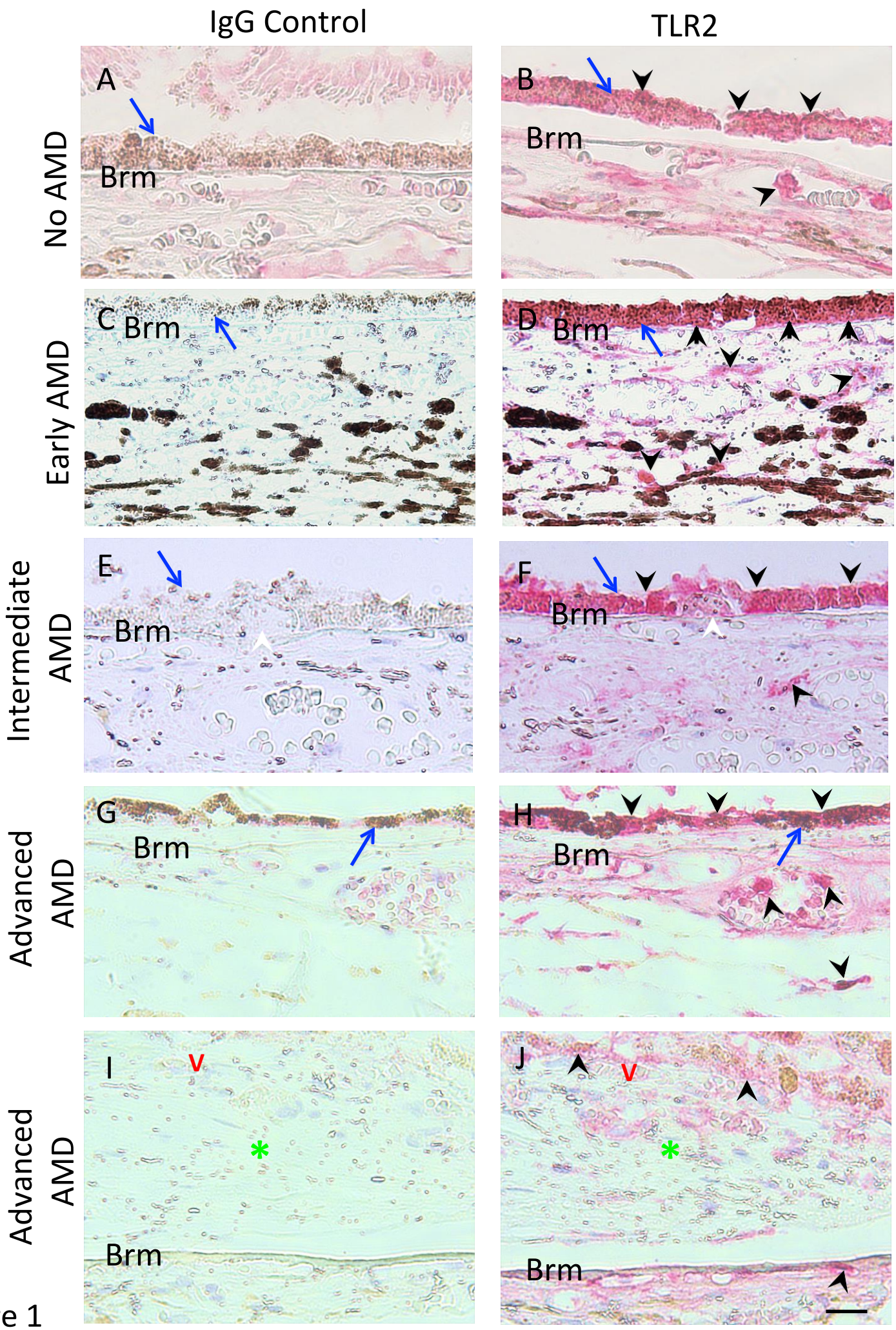
IgG Control
TLR2
No AMD
Early AMD
Intermediate AMD
Advanced AMD
Advanced AMD
A
B
C
D
E
F
G
H
I
J
Brm
Brm
Brm
Brm
Brm
Brm
Brm
Brm
Brm
Brm
V
V

Figure 1

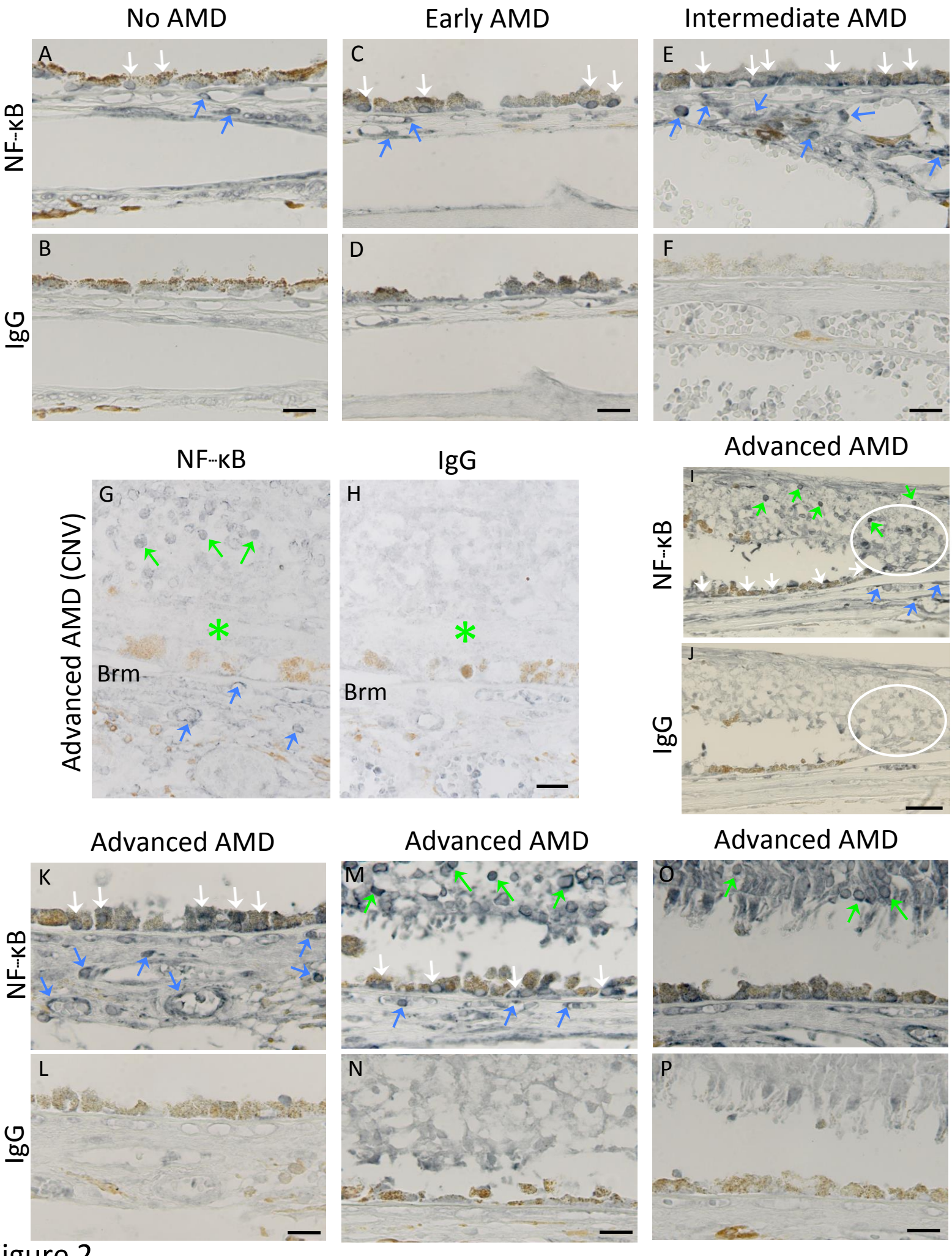
No AMD
Early AMD
Intermediate AMD
NF-κB
IgG
A
B
C
D
E
F
NF-κB
IgG
Advanced AMD
Advanced AMD (CNV)
G
H
I
J
Brm
Brm
NF-κB
IgG
Advanced AMD
Advanced AMD
Advanced AMD
K
L
M
N
O
P
NF-κB
IgG

Figure 2

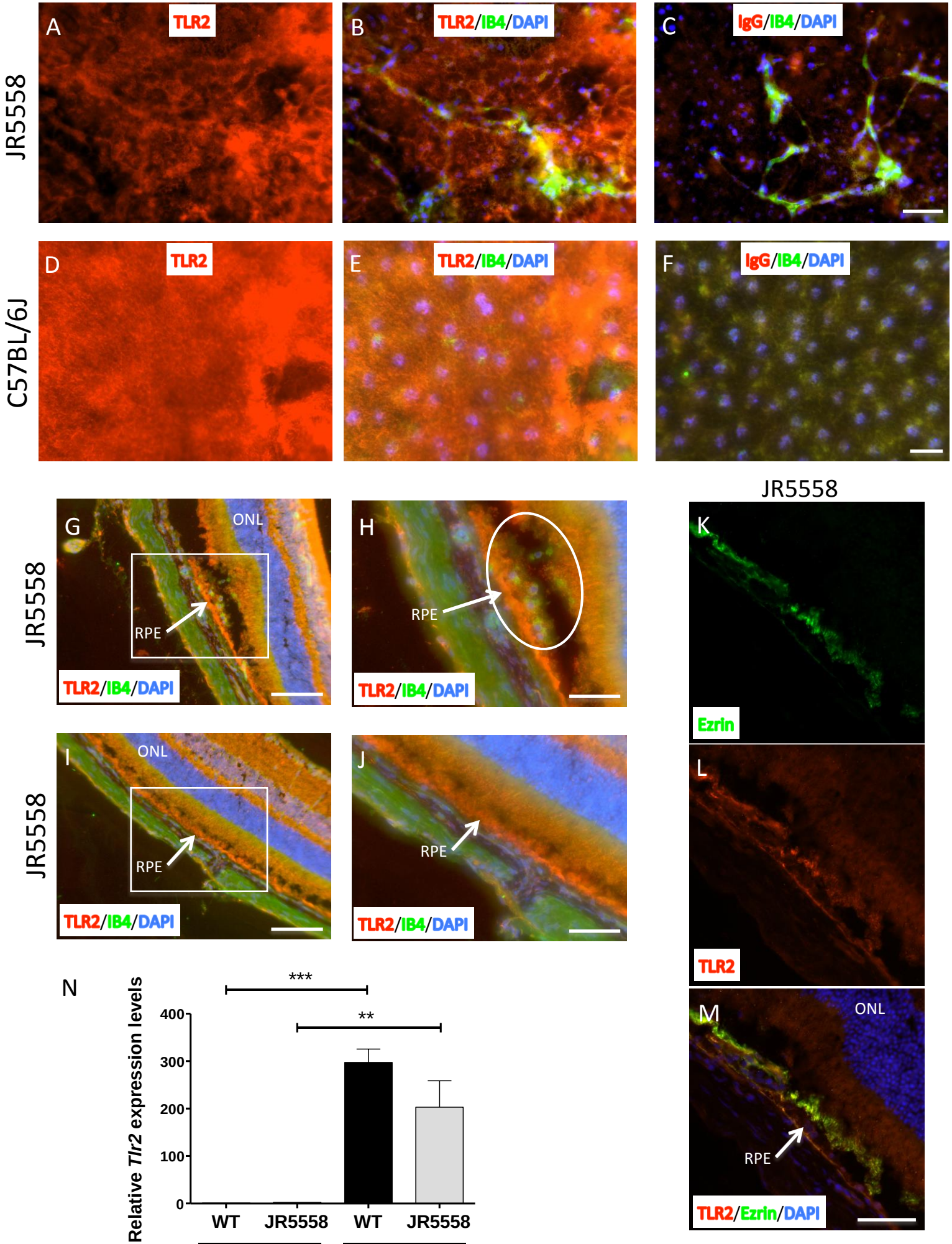
JR5558
A
TLR2
B
TLR2/IB4/DAPI
C
IgG/IB4/DAPI
C57BL/6J
D
TLR2
E
TLR2/IB4/DAPI
F
IgG/IB4/DAPI
JR5558
G
ONL
RPE
TLR2/IB4/DAPI
H
RPE
TLR2/IB4/DAPI
JR5558
I
ONL
RPE
TLR2/IB4/DAPI
J
RPE
TLR2/IB4/DAPI
JR5558
K
Ezrin
L
TLR2
M
ONL
RPE
TLR2/Ezrin/DAPI
N
Relative Tlr2 expression levels
***
**
400
300
200
100
0
WT
JR5558
WT
JR5558
Retina
RPE/Choroid

Figure 3

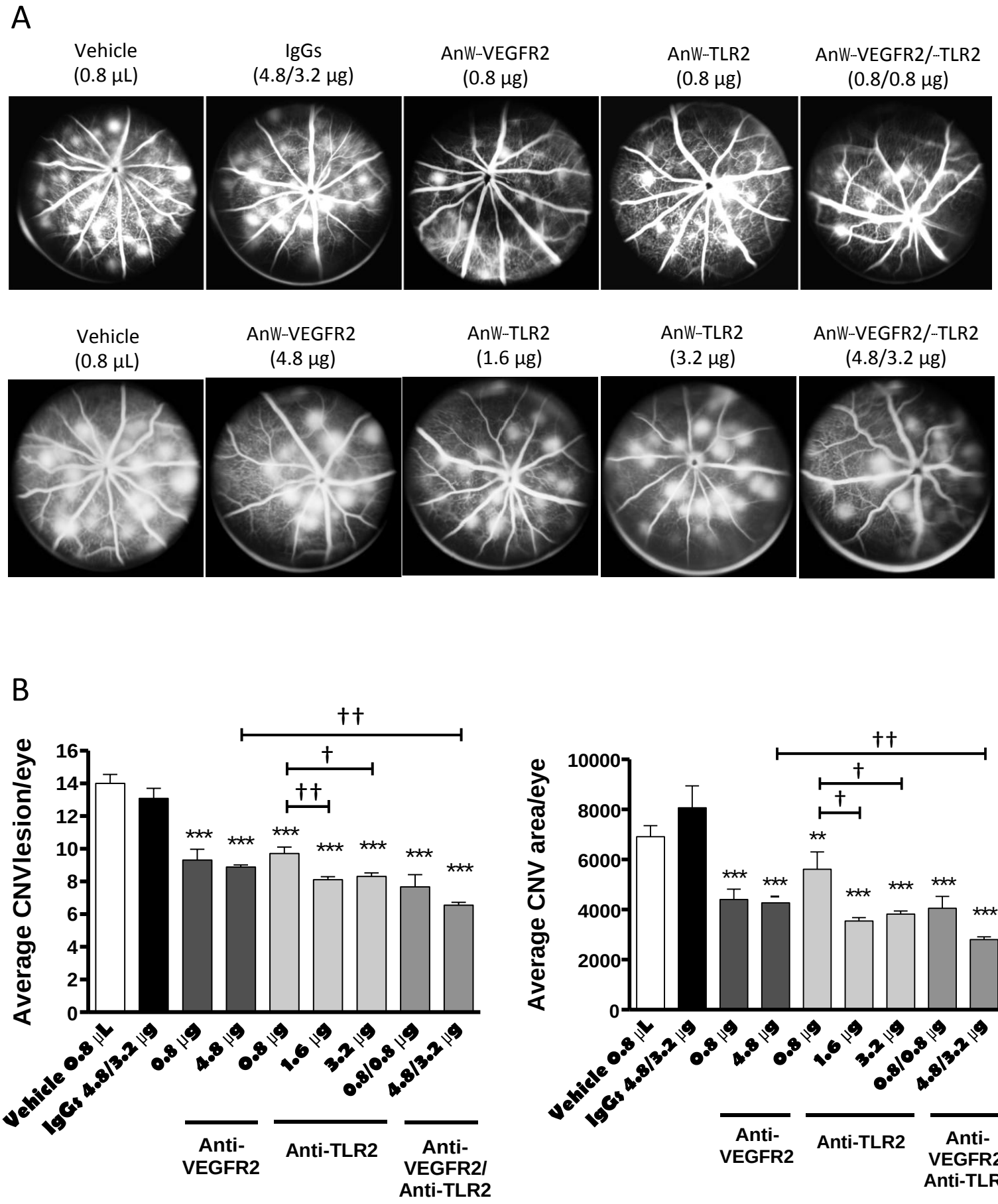
A
Vehicle (0.8 µL)
IgGs (4.8/3.2 µg)
AnW-VEGFR2 (0.8 µg)
AnW-TLR2 (0.8 µg)
AnW-VEGFR2/-TLR2 (0.8/0.8 µg)
Vehicle (0.8 µL)
AnW-VEGFR2 (4.8 µg)
AnW-TLR2 (1.6 µg)
AnW-TLR2 (3.2 µg)
AnW-VEGFR2/-TLR2 (4.8/3.2 µg)
B
Average CNVlesion/eye
Average CNV area/eye
Vehicle 0.8 µL
IgGs 4.8/3.2 µg
0.8 µg
4.8 µg
0.8 µg
1.6 µg
3.2 µg
0.8/0.8 µg
4.8/3.2 µg
Anti-VEGFR2
Anti-TLR2
Anti-VEGFR2/ Anti-TLR2

Figure 4

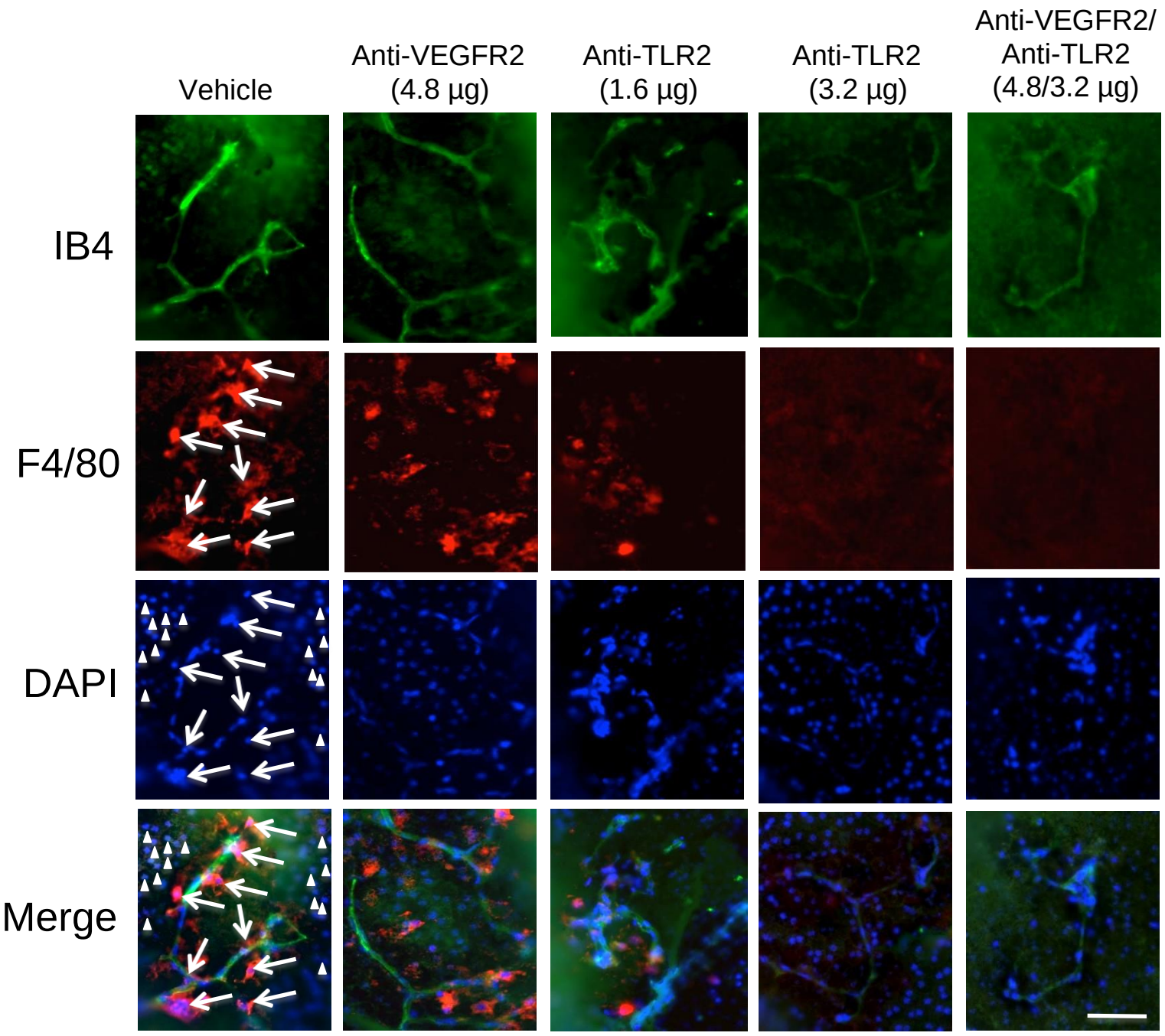
Vehicle
Anti-VEGFR2 (4.8 µg)
Anti-TLR2 (1.6 µg)
Anti-TLR2 (3.2 µg)
Anti-VEGFR2/ Anti-TLR2 (4.8/3.2 µg)
IB4
F4/80
DAPI
Merge

Figure 5

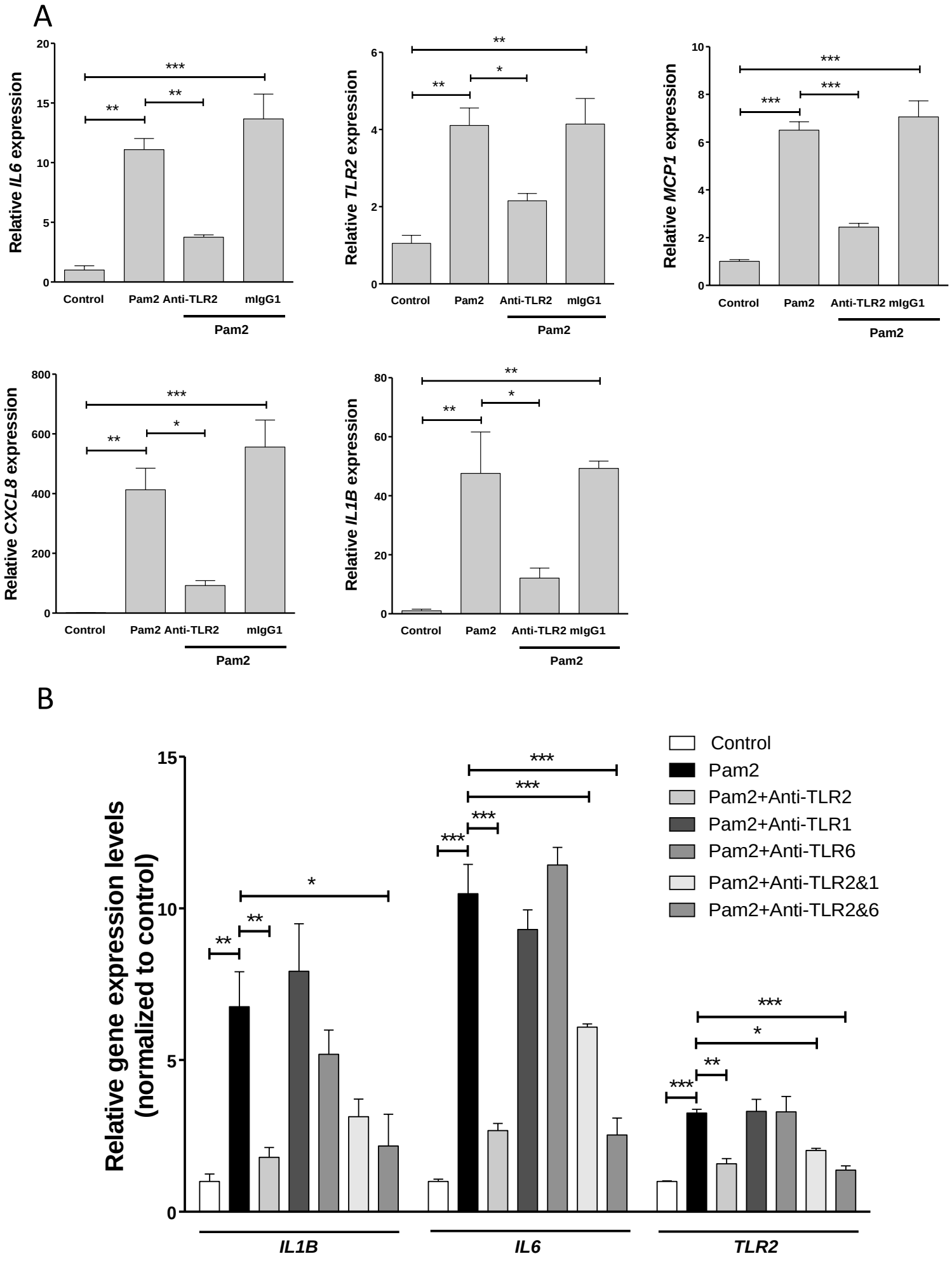
A
Relative IL6 expression
Control
Pam2
Anti-TLR2
mIgG1
Pam2
Relative TLR2 expression
Relative MCP1 expression
Relative CXCL8 expression
Relative IL1B expression
B
Relative gene expression levels (normalized to control)
Control
Pam2
Pam2+Anti-TLR2
Pam2+Anti-TLR1
Pam2+Anti-TLR6
Pam2+Anti-TLR2&1
Pam2+Anti-TLR2&6
IL1B
IL6
TLR2

Figure 6

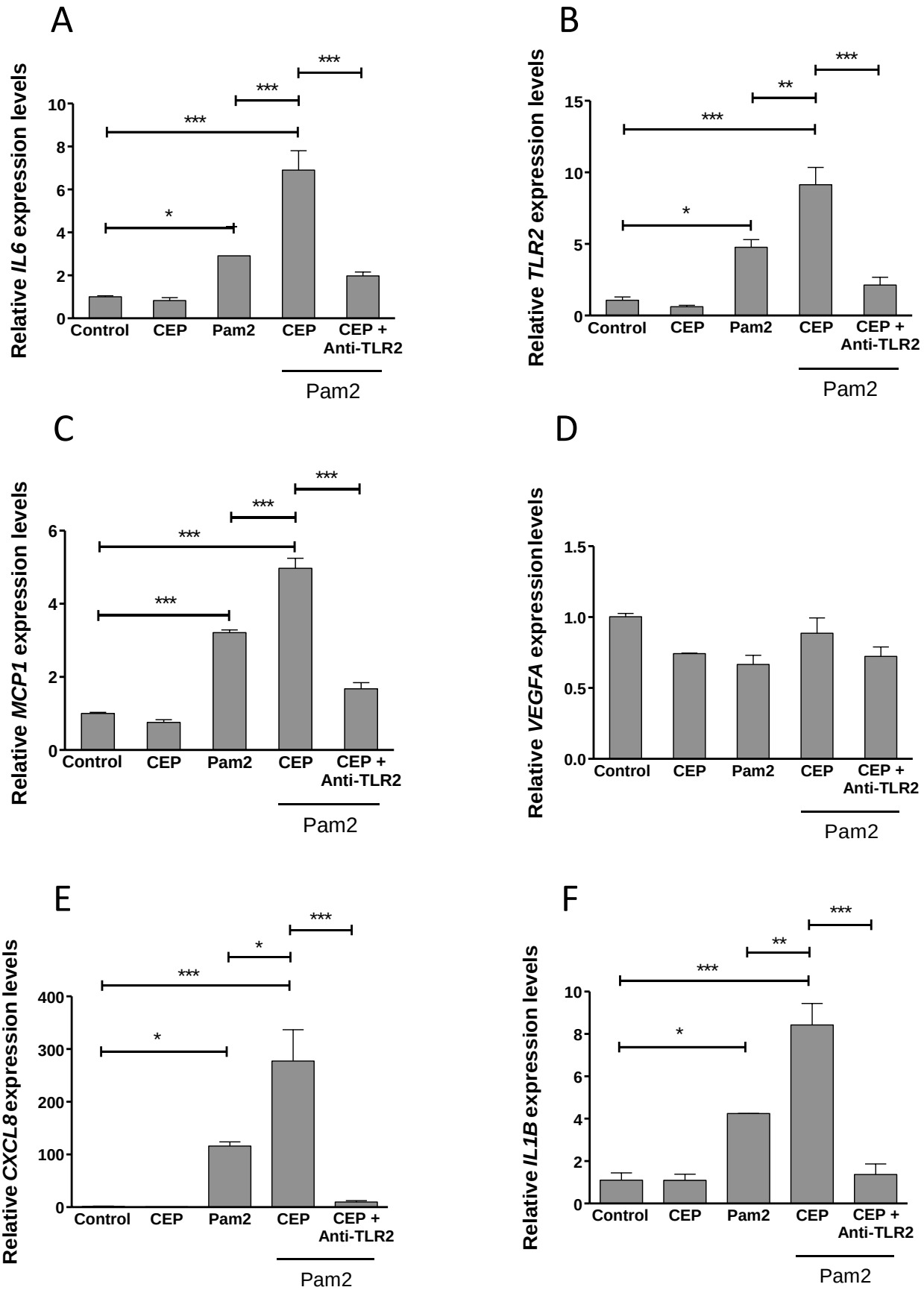
A
Relative IL6 expression levels
10
8
6
4
2
0
***
***
***
*
Control
CEP
Pam2
CEP
CEP + Anti-TLR2
Pam2
B
Relative TLR2 expression levels
15
10
5
0
***
**
***
*
Control
CEP
Pam2
CEP
CEP + Anti-TLR2
Pam2
C
Relative MCP1 expression levels
6
4
2
0
***
***
***
***
Control
CEP
Pam2
CEP
CEP + Anti-TLR2
Pam2
D
Relative VEGFA expression levels
1.5
1.0
0.5
0.0
Control
CEP
Pam2
CEP
CEP + Anti-TLR2
Pam2
E
Relative CXCL8 expression levels
400
300
200
100
0
***
*
***
*
Control
CEP
Pam2
CEP
CEP + Anti-TLR2
Pam2
F
Relative IL1B expression levels
10
8
6
4
2
0
***
**
***
*
Control
CEP
Pam2
CEP
CEP + Anti-TLR2
Pam2

Figure 7

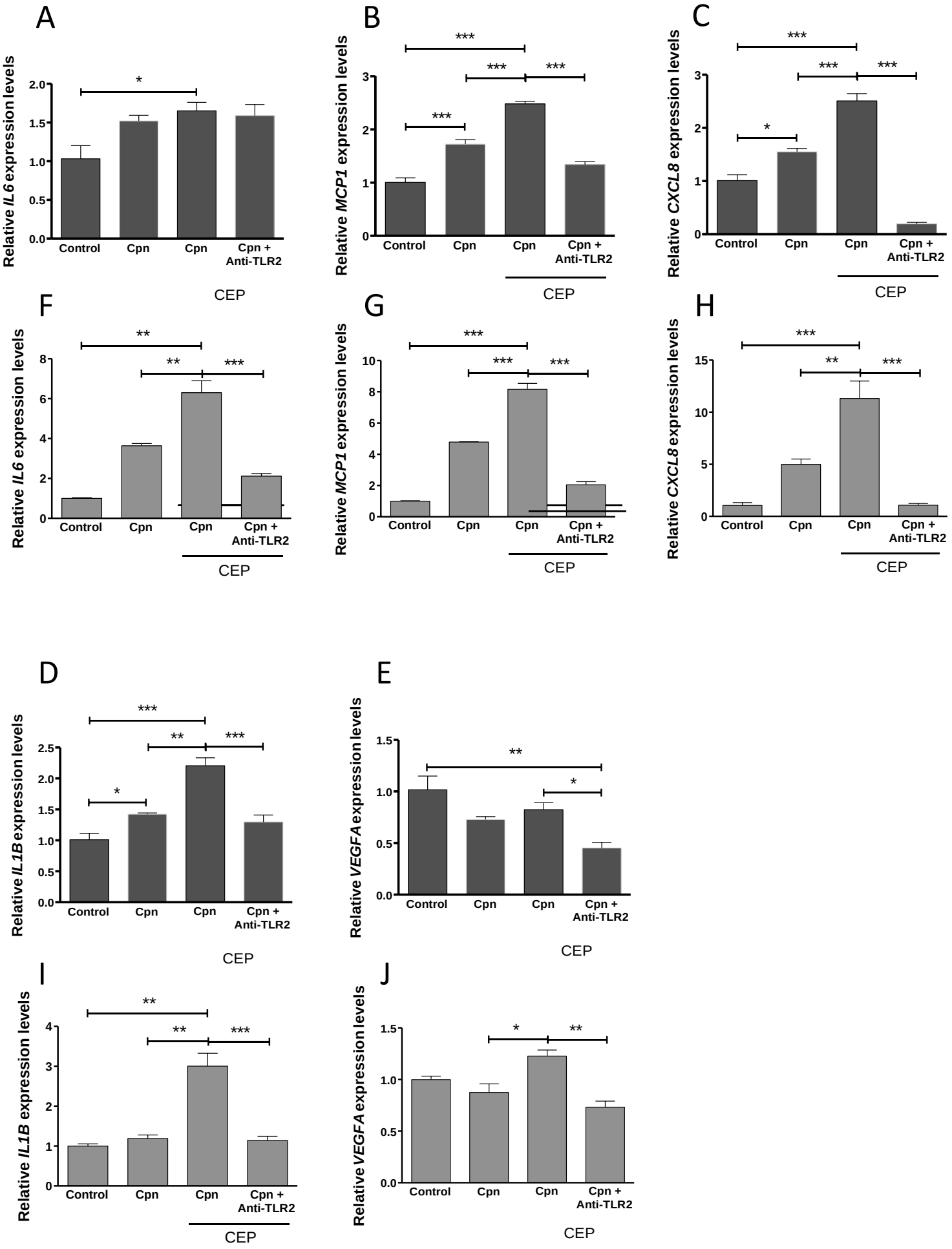
A
Relative IL6 expression levels
2.0
1.5
1.0
0.5
0.0
*
Control
Cpn
Cpn
Cpn + Anti-TLR2
CEP
B
Relative MCP1 expression levels
3
2
1
0
***
***
***
Control
Cpn
Cpn
Cpn + Anti-TLR2
CEP
C
Relative CXCL8 expression levels
3
2
1
0
***
***
***
*
Control
Cpn
Cpn
Cpn + Anti-TLR2
CEP
F
Relative IL6 expression levels
8
6
4
2
0
**
**
***
Control
Cpn
Cpn
Cpn + Anti-TLR2
CEP
G
Relative MCP1 expression levels
10
8
6
4
2
0
***
***
***
Control
Cpn
Cpn
Cpn + Anti-TLR2
CEP
H
Relative CXCL8 expression levels
15
10
5
0
***
**
***
Control
Cpn
Cpn
Cpn + Anti-TLR2
CEP
D
Relative IL1B expression levels
2.5
2.0
1.5
1.0
0.5
0.0
***
**
***
*
Control
Cpn
Cpn
Cpn + Anti-TLR2
CEP
E
Relative VEGFA expression levels
1.5
1.0
0.5
0.0
**
*
Control
Cpn
Cpn
Cpn + Anti-TLR2
CEP
I
Relative IL1B expression levels
4
3
2
1
0
**
**
***
Control
Cpn
Cpn
Cpn + Anti-TLR2
CEP
J
Relative VEGFA expression levels
1.5
1.0
0.5
0.0
*
**
Control
Cpn
Cpn
Cpn + Anti-TLR2
CEP

Figure 8

References

[1] Gragoudas ES, Adamis AP, Cunningham ET, Jr., Feinsod M, Guyer DR, Group VISiONCT: Pegaptanib for neovascular age-related macular degeneration. N Engl J Med 2004, 351:2805-16.

[2] Rosenfeld PJ, Brown DM, Heier JS, Boyer DS, Kaiser PK, Chung CY, Kim RY, Group MS: Ranibizumab for neovascular age-related macular degeneration. N Engl J Med 2006, 355:1419-31.

[3] Ferrara N, Gerber HP, LeCouter J: The biology of VEGF and its receptors. Nat Med 2003, 9:669-76.

[4] Ohno-Matsui K, Hirose A, Yamamoto S, Saikia J, Okamoto N, Gehlbach P, Duh EJ, Hackett S, Chang M, Bok D, Zack DJ, Campochiaro PA: Inducible expression of vascular endothelial growth factor in adult mice causes severe proliferative retinopathy and retinal detachment. The American journal of pathology 2002, 160:711-9.

[5] Okamoto N, Tobe T, Hackett SF, Ozaki H, Vinores MA, LaRochelle W, Zack DJ, Campochiaro PA: Transgenic mice with increased expression of vascular endothelial growth factor in the retina: a new model of intraretinal and subretinal neovascularization. The American journal of pathology 1997, 151:281-91.

[6] Oshima Y, Oshima S, Nambu H, Kachi S, Hackett SF, Melia M, Kaleko M, Connelly S, Esumi N, Zack DJ, Campochiaro PA: Increased expression of VEGF in retinal pigmented epithelial cells is not sufficient to cause choroidal neovascularization. Journal of cellular physiology 2004, 201:393-400.

[7] Schwesinger C, Yee C, Rohan RM, Joussen AM, Fernandez A, Meyer TN, Poulaki V, Ma JJ, Redmond TM, Liu S, Adamis AP, D'Amato RJ: Intrachoroidal neovascularization in transgenic mice overexpressing vascular endothelial growth factor in the retinal pigment epithelium. The American journal of pathology 2001, 158:1161-72.

659 [8] Comparison of Age-related Macular Degeneration Treatments Trials Research G,
660 Maguire MG, Martin DF, Ying GS, Jaffe GJ, Daniel E, Grunwald JE, Toth CA, Ferris
661 FL, 3rd, Fine SL: Five-Year Outcomes with Anti-Vascular Endothelial Growth Factor
662 Treatment of Neovascular Age-Related Macular Degeneration: The Comparison of
663 Age-Related Macular Degeneration Treatments Trials. Ophthalmology 2016,
664 123:1751-61.
665 [9] Kovach JL, Schwartz SG, Flynn HW, Jr., Scott IU: Anti-VEGF Treatment
666 Strategies for Wet AMD. J Ophthalmol 2012, 2012:786870.
667 [10] Rofagha S, Bhisitkul RB, Boyer DS, Sadda SR, Zhang K, Group S-US: Seven-
668 year outcomes in ranibizumab-treated patients in ANCHOR, MARINA, and
669 HORIZON: a multicenter cohort study (SEVEN-UP). Ophthalmology 2013, 120:2292-
670 9.
671 [11] Scott AW, Bressler SB: Long-term follow-up of vascular endothelial growth factor
672 inhibitor therapy for neovascular age-related macular degeneration. Curr Opin
673 Ophthalmol 2013, 24:190-6.
674 [12] Takeda AL, Colquitt J, Clegg AJ, Jones J: Pegaptanib and ranibizumab for
675 neovascular age-related macular degeneration: a systematic review. Br J Ophthalmol
676 2007, 91:1177-82.
677 [13] Foxton RH, Finkelstein A, Vijay S, Dahlmann-Noor A, Khaw PT, Morgan JE,
678 Shima DT, Ng YS: VEGF-A is necessary and sufficient for retinal neuroprotection in
679 models of experimental glaucoma. The American journal of pathology 2013,
680 182:1379-90.
681 [14] Nishijima K, Ng YS, Zhong L, Bradley J, Schubert W, Jo N, Akita J, Samuelsson
682 SJ, Robinson GS, Adamis AP, Shima DT: Vascular endothelial growth factor-A is a
683 survival factor for retinal neurons and a critical neuroprotectant during the adaptive
684 response to ischemic injury. The American journal of pathology 2007, 171:53-67.
685 [15] Saint-Geniez M, Maharaj AS, Walshe TE, Tucker BA, Sekiyama E, Kurihara T,
686 Darland DC, Young MJ, D'Amore PA: Endogenous VEGF is required for visual

687 function: evidence for a survival role on muller cells and photoreceptors. PloS one
688 2008, 3:e3554.
689 [16] Wang Y, Wang VM, Chan CC: The role of anti-inflammatory agents in age-
690 related macular degeneration (AMD) treatment. Eye (Lond) 2011, 25:127-39.
691 [17] Morohoshi K, Goodwin AM, Ohbayashi M, Ono SJ: Autoimmunity in retinal
692 degeneration: autoimmune retinopathy and age-related macular degeneration. J
693 Autoimmun 2009, 33:247-54.
694 [18] Edwards AO, Ritter R, 3rd, Abel KJ, Manning A, Panhuysen C, Farrer LA:
695 Complement factor H polymorphism and age-related macular degeneration. Science
696 2005, 308:421-4.
697 [19] Hageman GS, Anderson DH, Johnson LV, Hancox LS, Taiber AJ, Hardisty LI,
698 Hageman JL, Stockman HA, Borchardt JD, Gehrs KM, Smith RJ, Silvestri G, Russell
699 SR, Klaver CC, Barbazetto I, Chang S, Yannuzzi LA, Barile GR, Merriam JC, Smith
700 RT, Olsh AK, Bergeron J, Zernant J, Merriam JE, Gold B, Dean M, Allikmets R: A
701 common haplotype in the complement regulatory gene factor H (HF1/CFH)
702 predisposes individuals to age-related macular degeneration. Proceedings of the
703 National Academy of Sciences of the United States of America 2005, 102:7227-32.
704 [20] Haines JL, Hauser MA, Schmidt S, Scott WK, Olson LM, Gallins P, Spencer KL,
705 Kwan SY, Noureddine M, Gilbert JR, Schnetz-Boutaud N, Agarwal A, Postel EA,
706 Pericak-Vance MA: Complement factor H variant increases the risk of age-related
707 macular degeneration. Science 2005, 308:419-21.
708 [21] Klein RJ, Zeiss C, Chew EY, Tsai JY, Sackler RS, Haynes C, Henning AK,
709 SanGiovanni JP, Mane SM, Mayne ST, Bracken MB, Ferris FL, Ott J, Barnstable C,
710 Hoh J: Complement factor H polymorphism in age-related macular degeneration.
711 Science 2005, 308:385-9.
712 [22] Espinosa-Heidmann DG, Suner IJ, Hernandez EP, Monroy D, Csaky KG,
713 Cousins SW: Macrophage depletion diminishes lesion size and severity in

714 experimental choroidal neovascularization. Investigative ophthalmology & visual
715 science 2003, 44:3586-92.
716 [23] Lopez PF, Grossniklaus HE, Lambert HM, Aaberg TM, Capone A, Jr., Sternberg
717 P, Jr., L'Hernault N: Pathologic features of surgically excised subretinal neovascular
718 membranes in age-related macular degeneration. American journal of ophthalmology
719 1991, 112:647-56.
720 [24] Oh H, Takagi H, Takagi C, Suzuma K, Otani A, Ishida K, Matsumura M, Ogura
721 Y, Honda Y: The potential angiogenic role of macrophages in the formation of
722 choroidal neovascular membranes. Investigative ophthalmology & visual science
723 1999, 40:1891-8.
724 [25] Sakurai E, Anand A, Ambati BK, van Rooijen N, Ambati J: Macrophage depletion
725 inhibits experimental choroidal neovascularization. Investigative ophthalmology &
726 visual science 2003, 44:3578-85.
727 [26] Kaarniranta K, Salminen A: Age-related macular degeneration: activation of
728 innate immunity system via pattern recognition receptors. J Mol Med (Berl) 2009,
729 87:117-23.
730 [27] Kumar MV, Nagineni CN, Chin MS, Hooks JJ, Detrick B: Innate immunity in the
731 retina: Toll-like receptor (TLR) signaling in human retinal pigment epithelial cells. J
732 Neuroimmunol 2004, 153:7-15.
733 [28] Ambati J, Atkinson JP, Gelfand BD: Immunology of age-related macular
734 degeneration. Nat Rev Immunol 2013, 13:438-51.
735 [29] Gay NJ, Gangloff M: Structure and function of Toll receptors and their ligands.
736 Annu Rev Biochem 2007, 76:141-65.
737 [30] Oliveira-Nascimento L, Massari P, Wetzler LM: The Role of TLR2 in Infection
738 and Immunity. Front Immunol 2012, 3:79.
739 [31] West XZ, Malinin NL, Merkulova AA, Tischenko M, Kerr BA, Borden EC, Podrez
740 EA, Salomon RG, Byzova TV: Oxidative stress induces angiogenesis by activating
741 TLR2 with novel endogenous ligands. Nature 2010, 467:972-6.

[32] Grote K, Schutt H, Schieffer B: Toll-like receptors in angiogenesis. ScientificWorldJournal 2011, 11:981-91.

[33] Beatty S, Koh H, Phil M, Henson D, Boulton M: The role of oxidative stress in the pathogenesis of age-related macular degeneration. Survey of ophthalmology 2000, 45:115-34.

[34] Erridge C: Endogenous ligands of TLR2 and TLR4: agonists or assistants? Journal of leukocyte biology 2010, 87:989-99.

[35] Saeed AM, Duffort S, Ivanov D, Wang H, Laird JM, Salomon RG, Cruz-Guilloty F, Perez VL: The oxidative stress product carboxyethylpyrrole potentiates TLR2/TLR1 inflammatory signaling in macrophages. PloS one 2014, 9:e106421.

[36] Fujimoto T, Sonoda KH, Hijioka K, Sato K, Takeda A, Hasegawa E, Oshima Y, Ishibashi T: Choroidal neovascularization enhanced by Chlamydia pneumoniae via Toll-like receptor 2 in the retinal pigment epithelium. Investigative ophthalmology & visual science 2010, 51:4694-702.

[37] Zhu Y, Liang L, Qian D, Yu H, Yang P, Lei B, Peng H: Increase in peripheral blood mononuclear cell Toll-like receptor 2/3 expression and reactivity to their ligands in a cohort of patients with wet age-related macular degeneration. Mol Vis 2013, 19:1826-33.

[38] Kalayoglu MV, Bula D, Arroyo J, Gragoudas ES, D'Amico D, Miller JW: Identification of Chlamydia pneumoniae within human choroidal neovascular membranes secondary to age-related macular degeneration. Graefe's archive for clinical and experimental ophthalmology = Albrecht von Graefes Archiv fur klinische und experimentelle Ophthalmologie 2005, 243:1080-90.

[39] Nagai N, Ju M, Izumi-Nagai K, Robbie SJ, Bainbridge JW, Gale DC, Pierre E, Krauss AH, Adamson P, Shima DT, Ng YS: Novel CCR3 Antagonists Are Effective Mono- and Combination Inhibitors of Choroidal Neovascular Growth and Vascular Permeability. The American journal of pathology 2015, 185:2534-49.

769 [40] Nagai N, Lundh von Leithner P, Izumi-Nagai K, Hosking B, Chang B, Hurd R,
770 Adamson P, Adamis AP, Foxton RH, Ng YS, Shima DT: Spontaneous CNV in a
771 novel mutant mouse is associated with early VEGF-A-driven angiogenesis and late-
772 stage focal edema, neural cell loss, and dysfunction. Investigative ophthalmology &
773 visual science 2014, 55:3709-19.
774 [41] Doyle SL, Lopez FJ, Celkova L, Brennan K, Mulfaul K, Ozaki E, Kenna PF,
775 Kurali E, Hudson N, Doggett T, Ferguson TA, Humphries P, Adamson P, Campbell
776 M: IL-18 Immunotherapy for Neovascular AMD: Tolerability and Efficacy in
777 Nonhuman Primates. Investigative ophthalmology & visual science 2015, 56:5424-
778 30.
779 [42] Maminishkis A, Miller SS: Experimental models for study of retinal pigment
780 epithelial physiology and pathophysiology. Journal of visualized experiments : JoVE
781 2010.
782 [43] Zarember KA, Godowski PJ: Tissue expression of human Toll-like receptors and
783 differential regulation of Toll-like receptor mRNAs in leukocytes in response to
784 microbes, their products, and cytokines. Journal of immunology 2002, 168:554-61.
785 [44] Buwitt-Beckmann U, Heine H, Wiesmuller KH, Jung G, Brock R, Akira S, Ulmer
786 AJ: Toll-like receptor 6-independent signaling by diacylated lipopeptides. European
787 journal of immunology 2005, 35:282-9.
788 [45] Detrick B, Hooks JJ: Immune regulation in the retina. Immunologic research
789 2010, 47:153-61.
790 [46] Crabb JW, Miyagi M, Gu X, Shadrach K, West KA, Sakaguchi H, Kamei M,
791 Hasan A, Yan L, Rayborn ME, Salomon RG, Hollyfield JG: Drusen proteome
792 analysis: an approach to the etiology of age-related macular degeneration.
793 Proceedings of the National Academy of Sciences of the United States of America
794 2002, 99:14682-7.

795 [47] Gu X, Meer SG, Miyagi M, Rayborn ME, Hollyfield JG, Crabb JW, Salomon RG:
796 Carboxyethylpyrrole protein adducts and autoantibodies, biomarkers for age-related
797 macular degeneration. The Journal of biological chemistry 2003, 278:42027-35.
798 [48] Tseng WA, Thein T, Kinnunen K, Lashkari K, Gregory MS, D'Amore PA,
799 Ksander BR: NLRP3 inflammasome activation in retinal pigment epithelial cells by
800 lysosomal destabilization: implications for age-related macular degeneration.
801 Investigative ophthalmology & visual science 2013, 54:110-20.
802 [49] Cousins SW, Espinosa-Heidmann DG, Miller DM, Pereira-Simon S, Hernandez
803 EP, Chien H, Meier-Jewett C, Dix RD: Macrophage activation associated with
804 chronic murine cytomegalovirus infection results in more severe experimental
805 choroidal neovascularization. PLoS pathogens 2012, 8:e1002671.
806 [50] Miller DM, Espinosa-Heidmann DG, Legra J, Dubovy SR, Suner IJ, Sedmak DD,
807 Dix RD, Cousins SW: The association of prior cytomegalovirus infection with
808 neovascular age-related macular degeneration. American journal of ophthalmology
809 2004, 138:323-8.
810 [51] Wooten RM, Ma Y, Yoder RA, Brown JP, Weis JH, Zachary JF, Kirschning CJ,
811 Weis JJ: Toll-like receptor 2 is required for innate, but not acquired, host defense to
812 Borrelia burgdorferi. Journal of immunology 2002, 168:348-55.
813
814